Plant, Cell & Environment

Plant, Cell and Environment (2011) doi: 10.1111/j.1365-3040.2010.02269.x

Climate-related trends in sapwood biophysical properties in two conifers: avoidance of hydraulic dysfunction through coordinated adjustments in xylem efficiency, safety and capacitance

DAVID M. BARNARD[1,2]*, FREDERICK C. MEINZER[3], BARBARA LACHENBRUCH[2], KATHERINE A. MCCULLOH[2], DANIEL M. JOHNSON[4] & DAVID R. WOODRUFF[3]

[1]Department of Forest Ecosystems and Society, [2]Department of Wood Science and Engineering, Oregon State University, [3]USDA Forest Service, Forestry Sciences Laboratory, 3200 SW Jefferson Way, Corvallis, OR 97331 and [4]Department of Environmental and Plant Biology, Ohio University, Athens, OH 45701, USA

ABSTRACT

In the Pacific north-west, the Cascade Mountain Range blocks much of the precipitation and maritime influence of the Pacific Ocean, resulting in distinct climates east and west of the mountains. The current study aimed to investigate relationships between water storage and transport properties in populations of Douglas-fir (*Pseudotsuga menziesii*) and ponderosa pine (*Pinus ponderosa*) adapted to both climates. Sapwood thickness, capacitance, vulnerability to embolism, and axial and radial conductivity were measured on samples collected from trunks of mature trees. The sapwood of ponderosa pine was three to four times thicker than Douglas-fir. Radial conductivity was higher in west-side populations of both species, but axial conductivity was higher in the east-side populations and in Douglas-fir. Eastern populations of both species had sapwood that was more vulnerable to embolism than west-side populations. Sapwood capacitance was similar between species, but was about twice as great in east-side populations (580 kg m^{-3} MPa^{-1}) as in west-side populations (274 kg m^{-3} MPa^{-1}). Capacitance was positively correlated with both mean embolism pressure and axial conductivity across species and populations, suggesting that coordinated adjustments in xylem efficiency, safety and water storage capacity may serve to avoid embolism along a gradient of increasing aridity.

Key-words: drought; hydraulic architecture; hydraulic conductivity; water storage; xylem vulnerability; xylem embolism.

Correspondence: D. M. Barnard. Department of Horticulture and Landscape Architecture, Colorado State University, 111 Shepardson, 1173 Campus Delivery, Fort Collins, CO 805231173, USA. e-mail: dave.barnard@colostate.edu

*Current address: Department of Horticulture and Landscape Architecture, Colorado State University, Fort Collins, CO 80523, USA.

INTRODUCTION

Water flows through the xylem in a metastable state following a hydrostatic pressure gradient of increasing tension from roots to leaves. During periods of high transpirational demand and/or low soil moisture, the tension in the water column may reach a point at which a gas bubble can be pulled into a xylem conduit and expand to form an embolism that blocks water transport (Zimmerman 1983; Crombie, Milburn & Hipkins 1985). The increased tension caused by the partial loss of conductivity can generate a positive feedback loop resulting in runaway embolism (Tyree & Sperry 1988), catastrophic hydraulic failure and, ultimately, plant death (McDowell *et al*. 2008; Brodribb & Cochard 2009). In response to these circumstances, trees have evolved to have a suite of physiological, allometric and anatomical traits that reduce the risk of potential xylem dysfunction induced by high tensions in the water column. These include maintenance of small leaf area relative to sapwood area (Mencuccini & Grace 1994), the ability of stomata to regulate transpiration to reduce the tension gradient (Farquhar & Sharkey 1982; Mencuccini & Grace 1994; Saliendra, Sperry & Comstock 1995; Whitehead 1998; McDowell *et al*. 2008), capacitive discharge of water from sapwood and other tissues that buffers fluctuations in xylem tension (Waring & Running 1978; Waring, Whitehead & Jarvis 1979; Holbrook 1995; Phillips *et al*. 2003; Meinzer *et al*. 2003, 2006, 2008a; Čermák *et al*. 2007; Scholz *et al*. 2007) and decreased pit membrane pore diameter and other changes in pit geometry that increase resistance to air-seeded embolism (Hacke, Sperry & Pittermann 2004; Domec *et al*. 2006a, 2008).

The tracheids of conifer sapwood often display morphology that appears to have resulted from a trade-off of safety of water transport, often expressed as the xylem water potential associated with 50% loss of conductivity (Ψ_{50}), against the efficiency, in terms of xylem specific conductivity (k_s). The safety versus efficiency tradeoff arises from the geometry and characteristics of the bordered pit pairs connecting adjacent tracheids. Larger pit apertures, as well as

pit membrane pore size between the strands comprising the margo, result in higher pit conductance but simultaneously increase the risk of air-seeding as a result of reduced torus overlap at the pit aperture (Hacke *et al*. 2004; Domec, Gartner & Meinzer 2006b; Domec *et al*. 2008; Cochard *et al*. 2009). Consistent with this tradeoff, positive relationships have been shown between maximum sapwood k_s and Ψ_{50} in Norway spruce (Rosner *et al*. 2008), Douglas-fir (Domec *et al*. 2006b, 2008) and ponderosa pine (Domec & Gartner 2003). In contrast to pit structural characteristics that allow xylem conduits to withstand high tensions without becoming embolized, capacitance can contribute to hydraulic safety through avoidance of tensions that would normally provoke embolism (Hölttä *et al*. 2009; Meinzer *et al*. 2008a, 2009). Strong positive correlations between stem capacitance and Ψ_{50} noted in several angiosperm and coniferous species (Domec & Gartner 2002; Domec, Pruyn & Gartner 2005; Meinzer *et al*. 2008a) suggest that capacitance should be considered as another dimension of hydraulic safety (Pratt *et al*. 2007; Sperry, Meinzer & McCulloh 2008; Hölttä *et al*. 2009; Meinzer *et al*. 2008a, 2009, 2010). Given the evidence that the sapwood itself is the dominant source of tension-buffering capacitance (Čermák *et al*. 2007; Scholz *et al*. 2007; Meinzer *et al*. 2008a; Hölttä *et al*. 2009), species with thicker sapwood might be expected to have smaller axial tension gradients and greater radial conductivity than species with thinner sapwood to facilitate withdrawal and subsequent recharge of stored water from inner sapwood.

The mild and moist climate west of the Cascade Mountains in Oregon and Washington, as well as the semi-arid continental climate east of the Cascade Crest, present an opportunity to study variation in hydraulic traits exhibited by tree species with populations adapted to both climates. Here, we investigate sapwood thickness, axial and radial conductivity, resistance to embolism, and intrinsic sapwood water storage capacity in Douglas-fir and ponderosa pine, two tree species with different sapwood thicknesses that also have populations adapted to conditions east and west of the Cascade Crest. The populations of Douglas-fir adapted to the Pacific Northwest are the coastal Douglas-fir (*Pseudotsuga menziesii* (Mirb.) Franco var. *menziesii*) and the Rocky Mountain, or interior, Douglas-fir [*P. menziesii* (Mirb.) Franco var. *glauca* (Beissn.) Franco]. Coastal Douglas-fir ranges from the Pacific Ocean eastward to the crest of the Cascade Mountains, where precipitation can be three to five times greater than the areas east of the Cascade Crest to which the interior Douglas-fir is adapted (Burns & Honkala 1990). Ponderosa pine (*Pinus ponderosa* Dougl. Ex Laws.) is the most widely distributed pine in North America (Burns & Honkala 1990) with a range extending from the mid-western US west to the Willamette Valley in Oregon and from British Columbia south into northern Mexico. Both species can be found growing together on both sides of the Cascade Crest, but ponderosa pine typically extends into drier regions than Douglas-fir (McMinn 1952; Emmingham *et al*. 2005). Despite the more xeric range of ponderosa pine, numerous investigations have shown its xylem to be more vulnerable to embolism than that of Douglas-fir in branch segments (Piñol & Sala 2000; Stout & Sala 2003; Martinez-Vilalta, Sala & Piñol 2004), roots (Stout & Sala 2003) and trunk sapwood (Domec & Gartner 2002; Bouffier, Gartner & Domec 2003).

We hypothesized that the success of ponderosa pine in drier conditions is due in part to the larger fraction of cross-sectional area utilized for water transport in the stem. Our second hypothesis was that greater vulnerability to embolism in ponderosa pine, in comparison to Douglas-fir, would be offset by a greater contribution of sapwood capacitance to hydraulic safety. Our third hypothesis was that radial conductivity would be proportional to sapwood thickness, that is, greater radial transport efficiency would be necessary to allow access to the entire sapwood profile for water transport and storage, and thus ponderosa pine would have greater radial conductivity than Douglas-fir.

METHODS

Sites, plant material and sample preparation

This study focused on studying tree hydraulic characteristics of populations of Douglas-fir and ponderosa pine endemic to the eastern or western sides of the Cascade Crest. Overall, the region is characterized by dry summers both west and east of the Cascade Crest with the bulk of precipitation occurring during the fall, winter and spring, and falling mostly as snow east of the crest. Mean annual precipitation is about 280 mm across the three sites east of the Cascade Crest and 1250 mm across the two sites in Western Oregon (Table 1). For the purpose of this study, a population refers to a species (i.e. Douglas-fir or ponderosa pine) at a specific location (east or west).

To represent each of the four populations, two uneven-aged, naturally regenerated stands were selected at sites throughout Oregon. From each stand, we selected 12 trees for sampling that had a breast-height (1.3 m) diameter of 20–40 cm, similar crown sizes and an overall healthy appearance (lacking visible damage, and/or insect or disease infestation). From each tree we then collected two 5-mm-diameter increment cores at breast height, to a depth that included the pith, to characterize individual tree growth history. Cores were taken at 90° angles to one another. However, if the tree had a visible lean to the trunk or was growing on a hill, cores were taken at a 90° angle from the axis of lean and/or perpendicular to the slope of the hill to minimize possible inclusion of compression or opposite wood in the samples. For determination of water transport and storage properties we selected six trees from the twelve trees described above and, from each, took three 12-mm-diameter increment cores, again, sampling to avoid compression or opposite wood. Immediately after we removed the cores from the trees we used a pencil to mark the heartwood/sapwood boundary (determined by a marked change in translucency) and quickly sealed the cores into two nested plastic bags and placed them in an ice-filled cooler for transport to the lab.

Table 1. Locations, number of stands sampled and characteristics of sites used in this study. Mean annual precipitation and mean maximum and minimum temperatures are from the nearest city

	Species sampled	Number of stands	Nearest city	Latitude/Longitude	Elevation (m)	General site characteristics	Mean annual precipitation (mm)	Annual maximum and minimum temperatures (°C)
Eastern sites								
Ochoco National Forest	Douglas-fir	2	Mitchell	43.58, –121.22	1185	(1) 20° slope and (2) flat area, both with mixed Douglas-fir and ponderosa pine	290	30/–4
Pine Mountain	Ponderosa pine	1	Milican	43.77, –120.96	1400	Mixed ponderosa and lodgepole pine at desert fringe, flat area	300	27/–4
Deschutes National Forest	Ponderosa pine	1	La Pine	43.58, –121.22	1680	Pure ponderosa pine stand, flat area	260	29/–4.5
Western sites								
Cascade Timber Consulting Inc.	Douglas-fir	1	Sweet Home	44.37, –122.83	285	Mixed stand of grand-fir big leaf maple and Douglas-fir, gentle slope	1400	27/0.5
MacDonald-Dunn	Douglas-fir	1	Corvallis	44.62, –123.29	200	Mixed stand of Douglas-fir, big leaf maple and grand fir, flat area	1100	28/1
Cascade Timber Consulting Inc.	Ponderosa pine	2	Sweet Home	44.37, –122.83	285	(1) Pure ponderosa pine stand and (2) Mixed ponderosa pine and Douglas-fir, flat area	1400	27/0.5

Individual tree growth characteristics

We used the two 5-mm-diameter increment cores from all trees to estimate sapwood thickness, and then used a dissecting microscope to estimate number of growth rings at breast height (hereafter referred to as tree age), number of rings of sapwood and average annual basal growth increment. Values for the two cores were then averaged. Basal area growth rates were estimated to represent the sampled trees as the average annual basal growth increment, from tree diameter divided by the total number of growth rings.

Axial and radial specific conductivity

The sapwood in the 12-mm-diameter cores was cut into outer, middle and inner segments using razor blades. The core that was used for axial specific conductivity ($k_{s\text{-}ax}$) measurements was cut into segments 6 mm in length (radial direction), with outer segments extending from two growth rings from the cambium inward (to ensure that xylem was mature), middle segments centred half-way between the cambium and the heartwood-sapwood boundary, and inner segments extending outward from two growth rings external to the heartwood-sapwood boundary (to ensure that heartwood was excluded). These segments were then cut down to 10 mm × 5 mm × 5 mm (axial, tangential and radial, respectively) using a razor blade. We then shaved the sharp corners to produce a cylinder that was 5 mm in diameter. Pilot work comparing specific conductivity from sapwood segments that were 150–200-mm-long (axial direction) to that of the 10 mm segments (axial direction) found statistically indistinguishable results ($P = 0.31$, data not shown), justifying the use of 10-mm-long segments for this study. The second 12-mm-diameter core was used for radial conductivity ($k_{s\text{-}rad}$) measurements and the outer, middle, and inner segments excluded the same four growth rings listed above, and were cut to 10 mm lengths (radial direction).

All conductivity samples were then submerged in a perfusion solution consisting of 0.22 μm filtered and degassed, distilled water, adjusted to pH 2 with HCl (to retard bacterial and fungal growth) that was placed under partial vacuum overnight to remove any gas emboli. We used the high pressure flow meter (HPFM) method (Tyree *et al.* 1993; Yang & Tyree 1994) to determine $k_{s\text{-}ax}$ and $k_{s\text{-}rad}$. Pilot work showed that $k_{s\text{-}rad}$ decreased with increasing pressure differential up to about 0.15 MPa and then levelled off. However, once the pressure differential stabilized (about 10 min) $k_{s\text{-}rad}$ did not decrease further with time. In contrast, $k_{s\text{-}ax}$ increased with increasing pressure differential up to about 0.05 MPa, where it levelled off and then decreased sharply with time. Thus, radial samples were perfused for 10–15 min at a pressure of about 0.2 MPa, and axial samples were perfused for 1–5 min at a pressure of about 0.08 MPa. During perfusions, flow rate was estimated from the pressure drop across a capillary tube of known resistance, between a pressurized water tank and the sample. The flow meter was previously calibrated by determining flow rates

(kg s^{-1}) through capillary tubes of various diameters over a series of known pressure differentials. All samples were perfused with water at room temperature (23 °C).

Sapwood moisture release and capacitance

The third 12-mm-diameter core was used to generate sapwood moisture release and capacitance curves and to measure acoustic emissions during dehydration. Moisture release and capacitance measurements were made on a 10-mm-long segment (radial direction) cut from a 12-mm-long segment per tree that came from the location corresponding to previously observed and published regions of peak sap flow. The remaining 2 mm segment (a disc) was used for acoustic emissions (see further discussion). The peak of sap flow for pines, including ponderosa pine, occurs about one third of the distance inward from the cambium to the heartwood-sapwood boundary (Ford *et al*. 2004a,b; Meinzer 2010). The peak of sap flow in Douglas-fir typically occurs immediately inward from the cambium (Domec *et al*. 2006a).

The moisture release/capacitance samples were vacuum-infiltrated overnight with the perfusion solution described above. The samples were then removed from the solution and segment volume was estimated using the immersion method. Next, the samples were blotted with a paper towel to remove excess water, weighed and placed into the caps of screen-cage thermocouple psychrometer chambers (83 series; JRD Merrill Specialty Equipment, Logan, UT, USA). The cap was then joined with the chamber and sealed tightly. All psychrometer chambers were placed inside nested polyethylene plastic bags, which were submerged in an insulated water bath for 2 h to allow equilibration. Following equilibration, a 12-channel digital psychrometer meter (85 series; JRD Merrill Specialty Equipment) was used for determination of water release isotherms. Measurements were recorded every 20 min until water potential values stabilized. The samples were then removed from the chambers, weighed and allowed to partially air-dry. Air-drying intervals were set in accordance with the rate at which water evaporated from the samples, based on measurements of mass. As the samples approached the presumed inflection point of the moisture release curves, we shortened the intervals between sampling in an effort to clearly define the shape of the curve. Following the drying periods, samples were resealed into their chambers and the entire procedure was repeated until water potential readings reached about –4 MPa. We then removed the samples and placed them in a drying oven overnight at 70 °C for determination of oven dry mass and calculation of sample density (as dry mass per green volume). Recorded psychrometer values were transformed to water potential values based on calibration curves of solutions of known water potential. Relative water content (RWC) was then estimated for each sample at each recorded mass by the following equation

$$\mathrm{RWC} = \frac{W_\mathrm{f} - W_\mathrm{d}}{W_\mathrm{s} - W_\mathrm{d}} \tag{1}$$

where W_f is the fresh mass of the sample, W_d is the oven dry mass and W_s is the fully saturated mass of the sample. The values of relative water deficit (RWD = 1 – RWC) were plotted against mean values of water potential (Ψ_mean) and fit with a modified hyperbola using the following equation

$$\Psi_\mathrm{mean} = \frac{a * \mathrm{RWD}}{1 + b * \mathrm{RWD}} \tag{2}$$

to estimate moisture release parameters (Table 2). This relationship between Ψ_mean and RWD was then used to determine water potential of samples subjected to acoustic emissions analysis of xylem vulnerability curves (see below).

Capacitance (C) values were determined from sapwood moisture release curves for individual trees (Fig. 1) following the method described in Meinzer *et al*. (2003):

$$C = \frac{dW}{d\Psi_\mathrm{sw}} \tag{3}$$

where C is expressed on a sapwood volume basis (kg m^{-3} MPa^{-1}), dW is the cumulative weight of water released and $d\Psi_\mathrm{sw}$ is the change in sapwood water potential. Capacitance values were calculated by fitting linear regression lines to the initial, nearly linear, portion of the cumulative mass of water lost versus tissue water potential curve (Fig. 2). Cumulative mass of water released initially increases rapidly over a range of sapwood water potentials

Table 2. Parameters of best fit of Eqn 2 to sapwood moisture release data. These parameters were used in Eqn 2 to calculate water potential values for a given RWC

	Coefficient	Coefficient value	SE	F	*P*	r^2
Douglas-fir						
East	a	–1.186	0.178	–6.67	<0.0001	0.79
	b	–1.000	0.070	–14.25	<0.0001	
West	a	–0.778	0.100	–7.72	<0.0001	0.52
	b	–1.006	0.035	–29.01	<0.0001	
Ponderosa pine						
East	a	–0.683	0.1088	–6.27	<0.0001	0.85
	b	–0.981	0.0483	–20.31	<0.0001	
West	a	–1.917	0.15	–12.78	<0.0001	0.85
	b	–0.881	0.0424	–20.77	<0.0001	

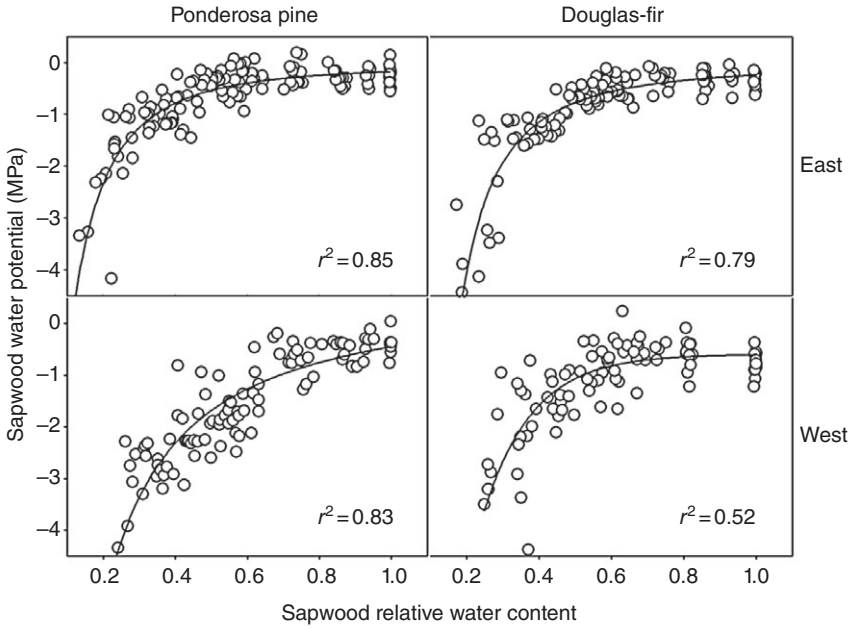

Figure 1. Moisture release curves of east-side and west-side populations of ponderosa pine and Douglas-fir show the relationship between sapwood water potential and relative water content.

corresponding to those normally experienced *in vivo* then slows and levels off at water potentials that typically correspond to the rapid accumulation of embolism (Meinzer *et al*. 2003, 2008a; Scholz *et al*. 2007).

Acoustic emissions and vulnerability to embolism parameters

For determination of sapwood vulnerability to embolism, we cut 2-mm-thick discs from the distal end of the section of the 12-mm-diameter core used to determine moisture release and capacitance (described earlier). A sliver in the axial-radial plane, about 6-mm-long (axially) and 3-mm-wide (tangentially), was cut from the edge of the disc, producing a piece of sapwood with the radial plane exposed on one side and the other side rounded. We then vacuum infiltrated the samples overnight in the perfusion solution (described above). Acoustic events were recorded by placing the radial plane flush against an acoustic sensor (R15α, Physical Acoustics Corporation, Princeton Junction, NJ, USA) connected to an ultrasonic acoustic emission (UAE)-specific data logger (either Pocket AE or USB AE node; Physical Acoustics Corporation). The acoustic sensor and sample were then held together with a clamp, an initial mass measurement was taken, and then the assembly was connected to the data logger and acoustically isolated from ambient noise.

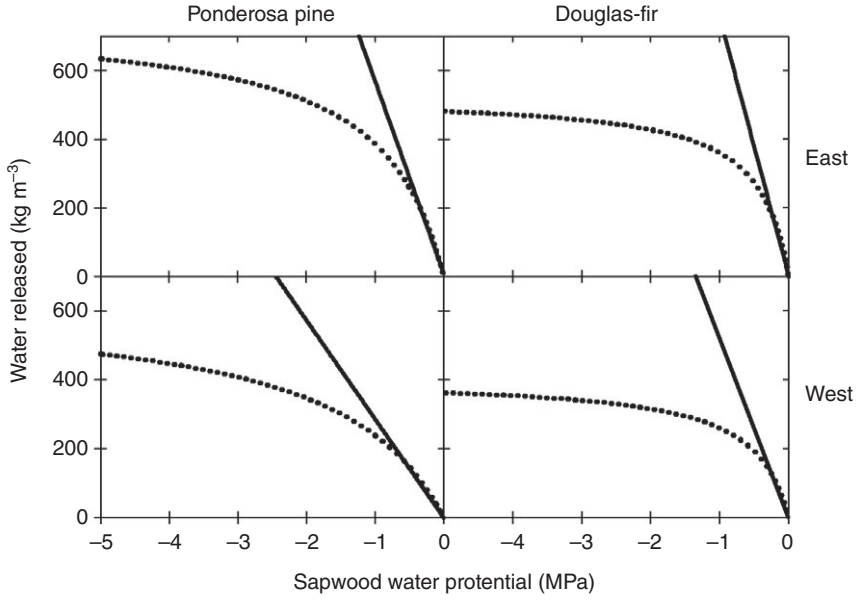

Figure 2. Representative graphs of capacitance show the relationship between the cumulative amount of water released (kg m^{-3}) and water potential in east-side and west-side populations of Douglas-fir and ponderosa pine. Capacitance values are calculated as the slope of the initial, nearly linear portion of the curve.

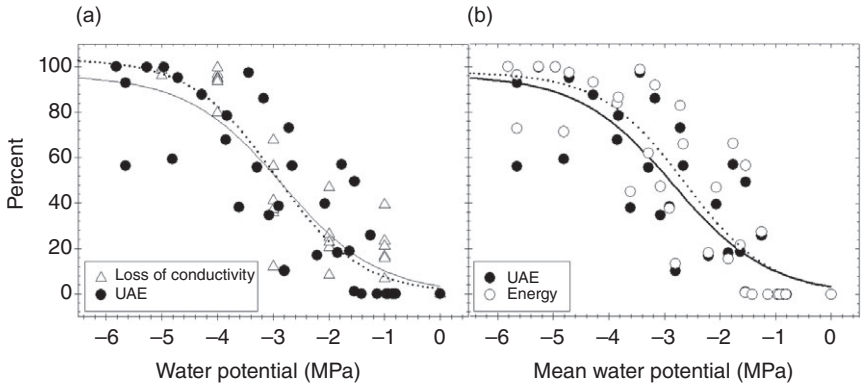

Figure 3. Comparison of (a) air injection (dotted line) and acoustic emissions (solid line) methods; and (b) cumulative acoustic events (UAE, solid line) and cumulative acoustic energy (dotted line) methods for determining vulnerability to embolism in sapwood sections of Douglas-fir. Note: water potential in (a) corresponds to negative of applied pressure for the air injection method and mean water potential values in (b) were derived from equations (1) and (2) in text.

The acoustic sensitivity threshold was set to a value of 45 dB. We allowed the samples to air-dry for a period ranging from 3 to 8 h while acoustic events were recorded continuously. At intervals ranging from 15 to 45 min (with the shorter intervals around presumed inflection points of the presumed sigmoidal curve), the clamp, sensor and sample assembly were disconnected from the data logger and mass and time from beginning of acoustic event acquisition recorded. We repeated this process until the rate of acoustic events slowed such that 10 min passed between individual acoustic events. We then removed the samples from the assembly and placed them in a 70 °C oven for 24 h. We determined percent of cumulative ultrasonic acoustic emissions (%UAE) and RWD (based on equation 1 above) for each interval during acquisition of acoustic events. We then used equation 2 above and the parameters in Table 2 to calculate mean water potential values (MPa) for each RWD value.

Numerous studies have demonstrated strong similarities between percent loss of conductivity (PLC: air injection pressure method) and %UAE in which a 50% loss of conductivity correlates with 50% UAE (Cochard 1992; Hacke & Sauter 1996; Rosner *et al*. 2006, 2008, 2009; Mayr & Rosner 2011). To ensure accuracy of this method for our species, we compared the traditional, pressure-sleeve, air-injection method with the acoustic emissions method. Additionally, we compared the shapes of the curves from cumulative energy and cumulative acoustic events (Fig. 3). In order to further characterize species and site differences in resistance to drought-induced embolism we calculated the values of the air entry threshold (Ψ_{AE}), mean embolism value (Ψ_{50}) and the full embolism point (Ψ_{FE}) (Pammenter & Vander Willigen 1998; Domec & Gartner 2002). To calculate Ψ_{AE} and Ψ_{FE} we fit a tangent line to the %UAE = 50 point of the sigmoidal curve. From the equation of this line we defined Ψ_{AE} as the water potential value at which the line crossed the *x*-axis and Ψ_{FE} as the water potential at which the regression line crossed the threshold at which %UAE equalled 100.

Statistical analysis

Within a population (east-side or west-side) site differences were not significant (two-sample *t*-test, $P > 0.2$ in all comparisons; data not shown), and thus all trees, from both stands of a population, were pooled together for analysis. This resulted in a sample of $n = 12$ trees for physiological analyses and $n = 24$ trees for growth characteristics of each population. Physiological and growth characteristics were analyzed using one-way and two-way analysis of variance. All comparisons were considered significant at the 95% confidence level. All statistical tests were done in S Plus (TIBICO Software, Palo Alto, CA, USA).

RESULTS

Growth characteristics

Sapwood thickness as a percentage of total stem diameter was three to four times greater in ponderosa pine than in Douglas-fir ($P < 0.001$), but differences in sapwood thickness were not significant between east and west-side populations ($P = 0.078$, Table 3). On the other hand, the percentage of growth rings included in the sapwood differed significantly by both species and site ($P > 0.001$) as did growth rates ($P < 0.001$ for both comparisons, Table 3), with west-side populations having thicker sapwood and growing faster than east-side populations, and ponderosa pine growing faster and having much thicker sapwood than Douglas-fir. Stem diameter at breast height was positively correlated with sapwood thickness ($P = 0.001$, $r^2 = 0.25$) but not with tree age ($P = 0.40$).

Hydraulic parameters

Capacitance (*C*) did not differ significantly between species in east-side or west-side populations ($P = 0.25$), but *C* was significantly higher in the east-side populations of both species ($P < 0.001$, Table 4). There was no significant relationship between *C* and early wood proportions across species ($P = 0.29$) but *C* did decrease significantly with increasing wood density across species ($P = 0.001$). Outer-$k_{s\text{-}ax}$ values were not significantly different between species ($P = 0.435$) but east-side populations of both species had significantly higher outer-$k_{s\text{-}ax}$ values than west-side populations ($P < 0.001$). East-side populations had significantly higher middle-$k_{s\text{-}ax}$ ($P = 0.009$) but showed

Table 3. General growth characteristics for sample populations including values of sapwood thickness, tree diameter, total sapwood thickness as a percentage of diameter at breast height (% SW Depth), tree age, number of growth rings included in sapwood, growth rings of sapwood as a percentage of the total number of growth rings (% Rings of SW), average annual basal growth increment at breast height (Growth Rate), and average sapwood density across three different sapwood depths. Different letters within a column indicate a significant difference at $P < 0.05$. Mean ± SE ($n = 24$)

	Sapwood thickness (cm)	Diameter (cm)	% SW depth	Age	Rings of sapwood	% rings of SW	Tree-specific growth rate (mm year^{-1})	Average sapwood density (g cm^{-13})
Douglas-fir								
East	3.5 ± 0.1a	37.4 ± 0.5a	18.4 ± 0.6a	99 ± 2a	32. ± 1a	32.3 ± 1.2a	8.3 ± 0.01a	0.39 ± 0.00a
West	2.7 ± 0.2b	33.4 ± 0.6b	15.9 ± 0.9a	62 ± 1b	10 ± 1b	17.6 ± 1.1b	13.1 ± 0.02b	0.45 ± 0.01b
Ponderosa pine								
East	12.9 ± 0.3 c	39.0 ± 0.6c	66.3 ± 1.4b	80 ± 3c	66 ± 2c	84.0 ± 2.0c	11.9 ± 0.02 c	0.47 ± 0.01 c
West	11.8 ± 0.5d	37.2 ± 0.3d	63.6 ± 2.3b	51 ± 1d	42 ± 2d	83.5 ± 2.3d	17.7 ± 0.03d	0.49 ± 0.01d

no significant difference between species ($P = 0.78$). In contrast, inner-$k_{s\text{-}ax}$ was significantly lower in east-side populations ($P = 0.03$) but again, there was no difference between species ($P = 0.23$). Overall, there was a marked decrease in $k_{s\text{-}ax}$ with increasing distance from the cambium independent of species or population (Fig. 4a). East-side populations of both species showed a greater decrease in $k_{s\text{-}ax}$, with increasing distance from the cambium than the west-side populations (Fig. 4a).

Overall, $k_{s\text{-}rad}$ was higher in west-side populations of both species ($P < 0.001$) at all three sapwood depths (Fig. 4b). Furthermore, west-side Douglas-fir had significantly higher $k_{s\text{-}rad}$ at all three sapwood depths than did ponderosa pine ($P = 0.009$, Fig. 4b). There was no significant difference in $k_{s\text{-}rad}$ between species in the east-side populations. ($P = 0.26$). In both east and west-side populations of Douglas-fir $k_{s\text{-}rad}$ peaked in the middle sections of the sapwood, whereas $k_{s\text{-}rad}$ increased inward from the cambium in west-side ponderosa pine and decreased inward from the cambium in east-side ponderosa pine.

Ψ_{AE} differed significantly among species and populations ($P < 0.001$) with west-side ponderosa pine having the lowest (most negative) Ψ_{AE} value (–2.1 MPa) and east-side Douglas-fir having the highest Ψ_{AE} (–1.0 MPa, Table 4, Fig. 5). There was no significant difference between Ψ_{50} of the species in east-side populations ($P = 0.23$) but in west-side populations, Ψ_{50} was significantly lower in both species ($P = 0.002$, Table 4, Fig. 6a), and significantly lower in ponderosa pine than Douglas-fir (Table 4). Both Ψ_{50} and $k_{s\text{-}ax}$ increased with sapwood C ($P < 0.001$, Fig. 6). Trends in Ψ_{50} and $k_{s\text{-}ax}$ with C were independent of species and population, but east-side populations of both species tended to have the highest values of C, Ψ_{50} and $k_{s\text{-}ax}$, and there was little overlap across populations.

DISCUSSION

The aim of this study was to compare sapwood water transport and storage characteristics in trunks of Douglas-fir and ponderosa pine. At first glance, it may seem paradoxical that the vulnerability of sapwood to embolism was highest for both species in the populations growing in the most arid sites. However, both capacitance and axial conductivity were also highest in these populations, suggesting that under dynamic conditions of high water loss from transpiration, these traits may play an important role in avoiding levels of xylem tension that would provoke excessive embolism in their more vulnerable trunk wood, compared to branch wood. The success of ponderosa pine in occupying drier areas than Douglas-fir is most likely associated with a larger suite of functional traits than those characterized here, but their end result seems to be to moderate xylem tension and embolism, thereby extending the period during which stomata are able to remain open for photosynthetic gas exchange. While our results on trunk sapwood may appear to run counter to the often reported trend of decreasing xylem vulnerability of terminal branches with increasing aridity, they highlight the need to measure xylem hydraulic

	Capacitance	Ψ_{AE}	Ψ_{50}	Ψ_{FE}
Douglas-fir				
East	572 ± 46a	–1.0 ± 0.2a	–2.0 ± 0.1a	–3.0 ± 0.3a
West	308 ± 19b	–1.6 ± 0.1b	–2.4 ± 0.1b	–3.7 ± 0.2b
Ponderosa pine				
East	586 ± 42a	–1.5 ± 0.2c	–2.0 ± 0.2a	–2.6 ± 0.2c
West	240 ± 24b	–2.1 ± 0.1d	–3.3 ± 0.1c	–4.4 ± 0.2d

Table 4. Values of capacitance (kg m^{-3} MPa^{-1}), air entry threshold (Ψ_{AE}, MPa) mean embolism pressure (Ψ_{50}) and full embolism pressure (Ψ_{FE}) in sapwood of east-side and west-side populations of Douglas-fir and ponderosa pine. Mean ± SE ($n = 12$). Values sharing the same letter within a column are not significantly different at $P < 0.05$

properties at multiple points along the root-to-leaf continuum to understand integrated suites of hydraulic traits contributing to overall drought resistance at the whole plant level (Meinzer *et al*. 2010).

Our first hypothesis proposed that greater sapwood thickness in ponderosa pine than in Douglas-fir would allow for the transport of water under lower tension in situations with similar evaporative demand and leaf area. Numerous examples in the literature indicate the relationship between leaf area and sapwood area can vary widely across species and with tree height (Grier & Waring 1974; Waring, Schroeder & Oren 1982; Mencuccini & Grace 1994; Gartner 2002; McDowell *et al*. 2002). Waring *et al*. (1982) calculated leaf area to sapwood area ratios for several conifer species to estimate crown leaf area from sapwood cross-sectional area and found a range of values from 0.14 up to 0.64 m^2 cm^{-2}. The ratios estimated for ponderosa pine and Douglas-fir were 0.25 m^2 cm^{-2} and 0.54 m^2 cm^{-2}, respectively. These ratios and our results suggest that compared to Douglas-fir, ponderosa pine has almost twice the sapwood area supplying water to a given leaf area. Darcy's law states that for porous materials, as cross-sectional area or k_s decreases, the pressure gradient required to drive a given amount of water must increase. Thus, a doubling of the sapwood cross-sectional area in relation to leaf area or a doubling of k_s at similar ratios of leaf area to sapwood area should lead to a 50% decrease in the pressure gradient

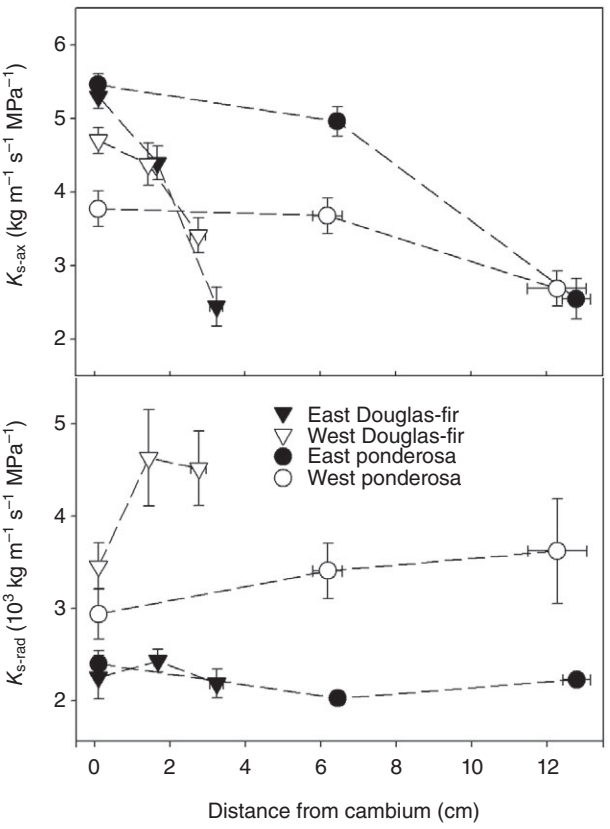

Figure 4. Radial profiles of axial ($k_{s\text{-}ax}$) and radial ($k_{s\text{-}rad}$) specific conductivities (kg m^{-1} s^{-1} MPa^{-1}) in east-side and west-side populations of ponderosa pine and Douglas-fir. Bars represent one standard error, $n = 12$.

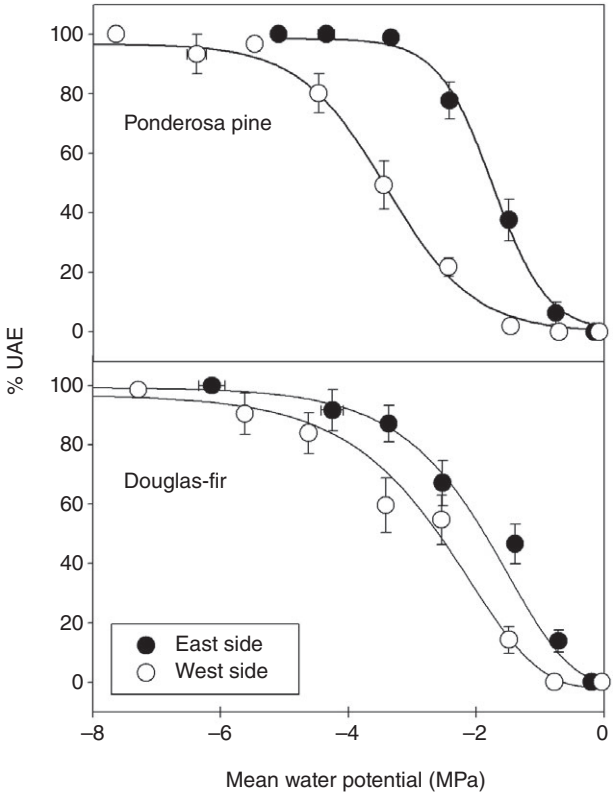

Figure 5. Vulnerability curves show the relationship between percent cumulative ultrasonic acoustic emissions (UAE) and mean water potential derived from moisture release data for ponderosa pine and Douglas-fir from east-side and west-side populations. Three-parameter, Sigmoidal curve fit to observational data. Bars represent one standard error $n = 12$.

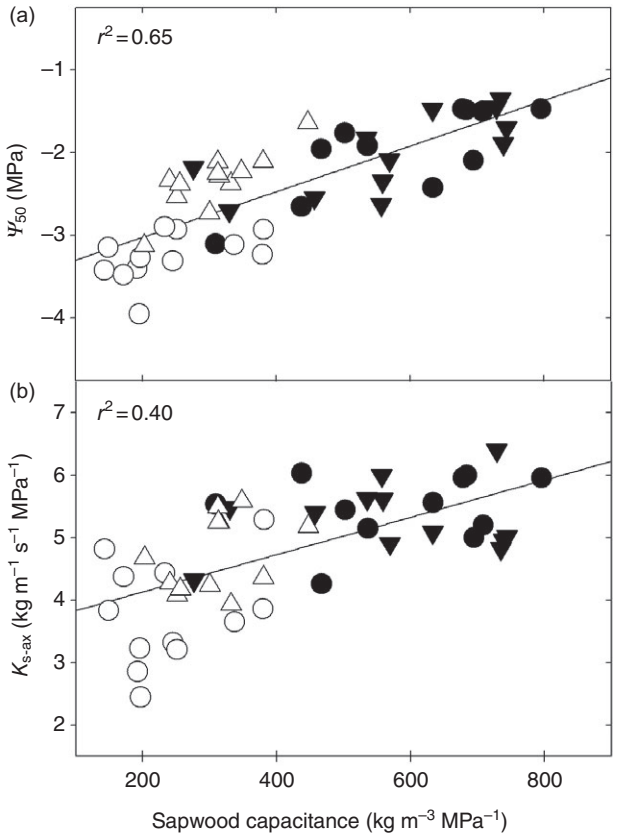

Figure 6. Relationships between sapwood capacitance and hydraulic parameters across species and populations. Upper panel (a) shows the relationship between sapwood capacitance and mean embolism pressure (Ψ_{50}); and (b) axial specific conductivity ($k_{s\text{-}ax}$). Each point represents a single tree.

required to conduct a given amount of water. Taken together, the lower leaf area to sapwood area ratio in ponderosa pine and its greater fraction of sapwood area per trunk cross-sectional area imply that trunks of ponderosa pine would operate at smaller maximum xylem tensions than Douglas-fir trunks (assuming similar stomatal responsiveness to environmental variables). Consistent with this prediction, Domec *et al*. (2009) estimated mean minimum *in situ* trunk xylem pressures of –1.5 and –2.1 MPa for old ponderosa pine and Douglas-fir trees, respectively.

Our second hypothesis that greater xylem vulnerability to embolism in ponderosa pine (compared to Douglas-fir) would be offset by a greater contribution of sapwood capacitance to its hydraulic safety, was not supported by the data: there were no significant differences between the species in their sapwood capacitance. However, capacitance in east-side populations of both species was about twice that of west-side populations. These site-specific differences in sapwood water storage and release characteristics were strongly and positively correlated with vulnerability to embolism (Fig. 6a) and suggest that daily discharge and refilling of water storage compartments in the drier east-side sides may offset the need for xylem structural modifications that would increase embolism resistance.

Although embolism may be a source of capacitive discharge of water into the transpiration stream, the resulting partial loss of xylem conductivity implies an increased risk of runaway embolism and potentially catastrophic xylem dysfunction (Tyree & Sperry 1988). Moreover, embolized conduits would need to be refilled on a daily basis in order for capacitance to remain constant over the normal physiological operating range of stem water potential. Nevertheless, modeling exercises suggest that water released into the transpiration stream by embolism can buffer water column tensions without a significant loss of overall conductivity and may help to avoid runaway embolism (Hölttä *et al*. 2009). In the present study, more than half of the capacitive discharge of water from trunk sapwood occurred at water potentials above –1 MPa in both east and west-side populations of both species (Fig. 2). Furthermore, the amount of water released from the air entry pressure to full embolism pressure was a small portion of total water released (Table 4). These data suggest that the contribution of water from embolism formation was insignificant compared to water stored and released at water potentials above air entry pressure that is held by capillarity or in elastic compartments such as sapwood axial or radial parenchyma.

The third hypothesis we addressed was that greater sapwood thickness would necessitate a higher $k_{s\text{-}rad}$ to allow for the radial movement of water between growth rings. This would appear to be of even greater importance in ponderosa pine and other pine species where the peak sap flow occurs up to about 1/3 of the distance inward from the cambium (Ford *et al*. 2004a,b; Meinzer 2010). In slower growing, east-side ponderosa pine, 1/3 of the distance inward from the cambium may constitute upwards of 100 years of growth and as many growth ring boundaries. Water must traverse these boundaries in order to reach the leaf trace connections, and ultimately the leaf–atmosphere interface (Maton & Gartner 2005). The required steady supply of water to support development in the cambial zone further necessitates a low resistance pathway for radial water movement. Overall, $k_{s\text{-}rad}$ values were not significantly different between species, and the west-side populations, which had thinner sapwood, also had higher $k_{s\text{-}rad}$ than the east-side populations of both species. The lower $k_{s\text{-}rad}$ values of east-side populations would appear to limit access to water stored in deeper portions of the sapwood because a steeper radial tension gradient would be required to sustain a given radial flux outward to the zones of greatest axial flow. With greater vulnerability to embolism in the east-side than west-side populations, it seems unlikely that east-side populations would experience those greater radial or axial tension gradients in their trunk sapwood. Lower $k_{s\text{-}rad}$ in east-side populations may be compensated by the greater capacitance of their sapwood, allowing substantially greater volumes of water to be extracted from storage for a given increase in tension (Table 4).

The preceding strategy, in droughty conditions, could prove to be particularly beneficial given the differences in soil properties and water availability between sites east and west of the Cascade Crest. For example, soils on the east-side tend to be sandier and have a lower organic content

than those on the west-side (Franklin & Dyrness 1973). Comparisons of soil moisture release curves for east and west-side sites show that within a normal physiological operating range of root water potential, a greater volume of water may be extracted from the sandier east-side soils for a given change of water potential than in west-side soils (Warren *et al*. 2005). However, there is a point of diminishing-returns at which further increases in xylem tensions may outpace the extraction of available water from the soil and act as a potential cause of air-seeded embolism. Upwards of 90% of available soil moisture may be lost in east side soils prior to a substantial drop in water potential (Warren *et al*. 2005), suggesting that a further reduction of xylem water potential would result in the uptake of a marginal amount of water, providing little selective pressure to invest energy into appropriate anatomical adjustments to increase resistance to tension-induced embolism. West side soils, on the other hand, experience a steeper decrease in their water potential at much higher available water contents than east-side soils resulting in a broader range of soil water potential over which it is physiologically feasible to extract water. West-side populations would thus be expected to show greater reliance on xylem anatomical traits associated with greater resistance to embolism. Consistent with this scenario and our results, Hacke *et al*. (2000) found that values of Ψ_{50} were less negative in roots and branches of *P. taeda* trees growing in sandy soil than in loamy soil.

In addition to differences in edaphic factors, differences in site elevation (in combination with the presence or absence of the maritime influence of the Pacific Ocean) and the resulting differences in annual minimum temperatures, may affect tree growth and play a role in the development of wood anatomy that favours resistance to freeze-induced embolism more strongly in east-side populations. Numerous examples in the literature indicate that larger tracheid diameters are directly correlated with greater vulnerability to freeze-induced embolism formation and that smaller tracheid diameters tend to be found in populations from more freeze-prone areas (Pittermann & Sperry 2003, 2006a,b). While tracheid diameter has been discussed as a potential regulator for drought-induced embolism formation, it has been mostly dismissed in favour of pit membrane structure and geometry (Hacke *et al*. 2004; Domec *et al*. 2006b, 2008; Cochard *et al*. 2009). However, in accordance with the Hagen–Poiseuille law, water flow through tracheids is a function of their radius to the fourth power, thus larger tracheids may conduct water more efficiently. While we made no direct measurements of tracheid diameters in this study, sample density may be used as a first-order approximation for comparing hypothetical tracheid diameters among samples (lower density wood indicates more lumen area and thus larger tracheids) from the same species. Our results indicate (by lower measured densities in east-side populations), that the higher conductivity values in east-side populations do coincide with lower sample density (and thus larger tracheid diameters. Furthermore, Mayr, Gruber & Bauer (2003) found that the occurrence of freeze-induced embolisms increased with the number of freeze-thaw events in conifers which suggests that west-side trees, most likely subject to more freeze–thaw events per season than east-side trees that are prone to longer periods of below freezing temperatures, may benefit from smaller tracheid lumen diameters by limiting embolism formation.

This study underscores the importance of understanding the interplay of water transport capacity, vulnerability to embolism and stem water storage. Embolism formation should be thought of differently from the risk of (or safety factor for) loss of whole-plant conductance. East-side populations adapted to more arid conditions exhibited less negative values of Ψ_{50} yet had higher values of capacitance indicating a coordinated adjustment to buffer excessive water column tensions, potentially preventing the formation of air-seeded embolism. Future studies would greatly benefit from increased understanding of the interactions between leaf-level controls of xylem tensions, the buffering capacity of the stem and the ability of the roots to supply water in relation to soil structure.

ACKNOWLEDGMENTS

We are grateful to Cascade Timber Consulting for supply of study material, to Peter Kitin and Steve Voelker, as well as to the two anonymous reviewers whose comments contributed greatly to this paper. This project was supported in part by the USDA Wood Utilization Research Special Grant to Oregon State University, by NSF grant 09–19871 and Joint Venture Agreement 07-JV-468 with the USDA Forest Service Pacific Northwest Research Station.

REFERENCES

Bouffier L.A., Gartner B.L. & Domec J.-C. (2003) Wood density and hydraulic properties of ponderosa pine from the Willamette Valley versus the Cascade Mountains. *Wood and Fiber Science* **35,** 217–233.

Brodribb T.J. & Cochard H. (2009) Hydraulic failure defines the recovery and point of death in water-stressed conifers. *Plant Physiology* 575–584.

Burns R.M. & Honkala B.H. (1990) *Silvics of North America: 1. Conifers*. Agriculture Handbook 654. Vol. 2. U.S. Department of Agriculture, Forest Service, Washington, DC, USA.

Čermák J., Kučera J., Bauerle W.L., Phillips N. & Hinckley T.M. (2007) Tree water storage and its diurnal dynamics related to sap flow and changes of stem volume in old-growth Douglas-fir trees. *Tree Physiology* **27,** 181–198.

Cochard H. (1992) Vulnerability of several conifers to embolism. *Tree Physiology* **11,** 73–83.

Cochard H., Hölttä T., Herbette S., Delzon S. & Mencuccini M. (2009) New insights into the mechanisms of water-stress-induced cavitations. *Plant Physiology* **151,** 949–954.

Crombie A.S., Milburn J.A. & Hipkins M.F. (1985) Maximum sustainable xylem tensions in *Rhododendron* and species. *Planta* **163,** 27–33.

Domec J.-C. & Gartner B.L. (2002) How do water transport and water storage differ in coniferous earlywood and latewood? *Journal of Experimental Botany* **53,** 2369–2379.

Domec J.-C. & Gartner B.L. (2003) Relationship between growth rates and xylem hydraulic characteristics in young, mature and

old-growth ponderosa pine trees. *Plant, Cell & Environment* **26,** 471–483.

Domec J.-C., Pruyn M.L. & Gartner B.L. (2005) Axial and radial profiles in conductivities, water storage and native embolism in trunks of young and old-growth ponderosa pine trees. *Plant, Cell & Environment* **28,** 1103–1113.

Domec J.-C., Meinzer F.C., Gartner B.L. & Woodruff D. (2006a) Transpiration-induced axial and radial tension gradients in trunks of Douglas-fir trees. *Tree Physiology* **26,** 275–284.

Domec J.-C., Gartner B.L. & Meinzer F.C. (2006b) Bordered pit structure and function determine spatial patterns of air-seeding thresholds in xylem of Douglas-fir (*Pseudotsuga menziesii*; Pinaceae) trees. *American Journal of Botany* **93,** 1588–1600.

Domec J.-C., Lachenbruch B., Meinzer F.C., Woodruff D.R., Waren J.M. & McCulloh K.A. (2008) Maximum height in a conifer is associated with conflicting requirements for xylem design. *Proceedings of the National Academy of Sciences of the United States of America* **105,** 12069–12074.

Domec J.-C., Warren J.M., Meinzer F.C. & Lachenbruch B. (2009) Safety factors for xylem failure by implosion and air-seeding within roots, trunks and branches of young and old conifer trees. *International Association of Wood Anatomists* **30,** 100–120.

Emmingham W.H., Oester P.T., Fitzgerald S.A., Filip G.M. & Edge W.D. (2005) *Ecology and Management of Eastern Oregon Forests*. Oregon State University Extension Service, Corvallis, OR, USA.

Farquhar G.D. & Sharkey T.D. (1982) Stomatal conductance and photosynthesis. *Annual Review of Plant Physiology* **33,** 317–345.

Ford C.R., Goranson C.E., Mitchell R.J., Will R.E. & Tesky R.O. (2004a) Diurnal and seasonal variability in the radial distribution of sap flow: predicting total stem flow in *Pinus taeda* trees. *Tree Physiology* **24,** 951–960.

Ford C.R., McGuire M.A., Mitchell R.J. & Tesky R.O. (2004b) Assessing variation in the radial profile of sap flux density in *Pinus* species and its effect on daily water use. *Tree Physiology* **24,** 241–249.

Franklin J.F. & Dyrness C.T. (1973) *Natural Vegetation of Oregon and Washington. General Technical Report PNW-8*. United States Department of Agriculture, Forest Service, Washington D.C., USA.

Gartner B.L. (2002) Sapwood and inner bark quantities in relation to leaf area and wood density in Douglas-fir. *International Association of Wood Anatomists* **23,** 267–285.

Grier C.C. & Waring R.H. (1974) Conifer foliage mass related to sapwood area. *Forest Science* **20,** 205–206.

Hacke U. & Sauter J.J. (1996) Drought-induced xylem dysfunction in petioles, branches, and roots of *Populus balsamifera* L. and *Alnus glutinosa* (L.) Gaertn. *Plant Physiology* **111,** 413–417.

Hacke U., Sperry J.S., Ewers B.E., Ellsworth D.S., Scafer K.V.R. & Oren R. (2000) Influence of soil porosity on water use in *Pinus taeda*. *Oecologia* **124,** 495–505.

Hacke U., Sperry J.S. & Pittermann J. (2004) Analysis of circular bordered pit function II. Gymnosperm tracheids with torus-margo pit membranes. *American Journal of Botany* **91,** 386–400.

Holbrook N.M. (1995) Stem water storage. In *Plant Stems: Physiology and Functional Morphology* (ed. B.L. Gartner), pp. 151–174. Academic Press, San Diego.

Hölttä T., Cochard H., Nikinmaa E. & Mencuccini M. (2009) Capacitive effect of cavitation in xylem conduits: results from a dynamic model. *Plant, Cell & Environment* **32,** 10–21.

Martinez-Vilalta J., Sala A. & Piñol J. (2004) The hydraulic architecture of Pinaceae – a review. *Plant Ecology* **171,** 3–13.

Maton C. & Gartner B.L. (2005) Do gymnosperm needles pull water through the xylem produced in the same year as the needle? *American Journal of Botany* **92,** 123–131.

Mayr S. & Rosner S. (2011) Cavitation in dehydrating xylem of Picea abies: energy properties of ultrasonic emissions reflect tracheid dimensions. *Tree Physiology* in press.

Mayr S., Gruber A. & Bauer H. (2003) Repeated freeze-thaw cycles induce embolism in drought stressed conifers (Norway spruce, stone pine). *Planta* **217,** 436–441.

McDowell N., Barnard H., Bond B.J., *et al*. (2002) The relationship between tree height and leaf area: sapwood area ratio. *Oecologia* **132,** 12–20.

McDowell N., Pockman W., Allen C., Breshears D.D., Cobb N., Kolb T., Sperry J.S., West A., Williams D. & Yepez E. (2008) Mechanisms of plant survival and mortality during drought: why do some plants survive while others succumb to drought? *The New Phytologist* **178,** 719–739.

McMinn R.G. (1952) The role of soil drought in the distribution of vegetation in the Northern Rocky Mountains. *Ecology* **33,** 1–15.

Meinzer F.C., James S.A., Goldstein G. & Woodruff D. (2003) Whole-tree water transport scales with sapwood capacitance in tropical forest canopy trees. *Plant, Cell & Environment* **26,** 1147–1155.

Meinzer F.C., Brooks J.R., Domec J.-C., Gartner B.L., Warren J.M., Woodruff D.R., Bible K. & Shaw D.C. (2006) Dynamics of water transport and storage in conifers studied with deuterium and heat tracing techniques. *Plant, Cell & Environment* **29,** 105–114.

Meinzer F.C., Woodruff D.R., Domec J.-C., Goldstein G., Campanello P.I., Giatti M.G. & Villalobos-Vega R. (2008a) Coordination of leaf and stem water transport properties in tropical forest trees. *Oecologia* **156,** 31–41.

Meinzer F.C., Johnson D.M., Lachenbruch B., McCulloh K.A. & Woodruff D.R. (2009) Xylem hydraulic safety margins in woody plants: coordination of stomatal control of xylem tension with hydraulic capacitance. *Functional Ecology* **23,** 922–930.

Meinzer F.C., McCulloh K.A., Lachenbruch B., Woodruff D.R. & Johnson D.M. (2010) The blind men and the elephant: the impact of context and scale in evaluating conflicts between plant hydraulic safety and efficiency. *Oecologia* **164,** 287–296.

Mencuccini M. & Grace J. (1994) Climate influences the leaf-area-sapwood area relationship in Scots pine (*Pinus sylvestris* L. *Tree Physiology* **15,** 1–10.

Pammenter N.W. & Vander Willigen C. (1998) A mathematical and statistical analysis of the curves illustrating vulnerability of xylem to cavitation. *Tree Physiology* **18,** 589–593.

Phillips N.G., Ryan M.G., Bond B.J., McDowell N.G., Hinckley T.M. & Čermák J. (2003) Reliance on stored water increases with tree size in three species in the Pacific Northwest. *Tree Physiology* **23,** 237–245.

Piñol J. & Sala A. (2000) Ecological implications of xylem cavitation for several Pinaceae in the Pacific Northwest. *Functional Ecology* **14,** 538–545.

Pittermann J. & Sperry J.S. (2003) Tracheid diameter is the key trait in determining the extent of freezing-induced embolisms in conifers. *Tree Physiology* **23,** 907–914.

Pittermann J. & Sperry J.S. (2006a) Mechanical reinforcement of tracheids compromises the hydraulic efficiency of conifer xylem. *Plant, Cell & Environment* **29,** 1618–1628.

Pittermann J. & Sperry J.S. (2006b) Analysis of freeze-thaw embolism in conifers. The interaction between cavitation pressure and tracheid size. *Plant Physiology* **140,** 374–382.

Pratt R.B., Jacobsen A.L., Ewers F.W. & Davis S.D. (2007) Relationships among xylem transport, biomechanics and storage in stems and roots of nine Rhamnaceae species of the California chaparral. *New Phytologist* **174,** 787–798.

Rosner S., Klein A., Wimmer R. & Karlsson B. (2006) Extraction of features from ultrasound acoustic emissions: a tool to assess the hydraulic vulnerability of Norway spruce trunkwood? *New Phytologist* **171,** 105–116.

Rosner S., Klein A., Müller U. & Karlsson B. (2008) Tradeoffs between hydraulic and mechanical stress responses of mature Norway spruce trunk wood. *Tree Physiology* **28,** 1179–1188.

Rosner S., Karlsson B., Konnerth J. & Hansmann C. (2009) Shrinkage processes in standard-size Norway spruce wood specimens with different vulnerability to cavitation. *Tree Physiology* **29,** 1419–1431.

Saliendra N.Z., Sperry J.S. & Comstock J.P. (1995) Influence of leaf water status on stomatal response to humidity, hydraulic conductance and soil drought in *Betula occidentalis*. *Planta* **196,** 357–366.

Scholz F.G., Bucci S.J., Goldstein G., Meinzer F.C., Franco A.C. & Miralles-Wilhelm F. (2007) Biophysical properties and functional significance of stem water storage tissues in Neotropical savanna trees. *Plant, Cell & Environment* **30,** 236–248.

Sperry J.S., Meinzer F.C. & McCulloh K.A. (2008) Safety and efficiency conflicts in hydraulic architecture: scaling from tissues to trees. *Plant, Cell & Environment* **31,** 632–645.

Stout D.L. & Sala A. (2003) Xylem vulnerability to cavitation in *Pseudotsuga meinziesii* and *Pinus ponderosa* from contrasting habitats. *Tree Physiology* **23,** 43–50.

Tyree M.T. & Sperry J.S. (1988) Do woody plants operate near the point of catastrophic xylem dysfunction caused by dynamic water stress? *Plant Physiology* **88,** 574–580.

Tyree M.T., Sinclair B., Lu P. & Granier A. (1993) Whole shoot hydraulic resistance in *Quercus* species measured with a new high pressure flow meter. *Annals of Forest Science* **50,** 417–423.

Waring R.H. & Running S.W. (1978) Sapwood water storage: its contribution to transpiration and effect upon water conductance through the stems of old-growth Douglas-fir. *Plant, Cell & Environment* **1,** 131–140.

Waring R.H., Whitehead D. & Jarvis P.G. (1979) The contribution of stored water to transpiration in Scots pine. *Plant, Cell & Environment* **2,** 309–317.

Waring R.H., Schroeder P.E. & Oren R. (1982) Application of the pipe model theory to predict canopy leaf area. *Canadian Journal of Forest Research* **12,** 556–560.

Warren J.M., Meinzer F.C., Brooks J.R. & Domec J.-C. (2005) Vertical stratification of soil water storage and release dynamics in Pacific Northwest coniferous forests. *Agricultural and Forest Meteorology* **130,** 39–58.

Whitehead D. (1998) Regulation of stomatal conductance and transpiration in forest canopies. *Tree Physiology* **18,** 633–644.

Yang S.D. & Tyree M.T. (1994) Hydraulic architecture of *Acer saccharum* and *A. rubrum*: comparison of branches to whole trees and the contribution of leaves to hydraulic resistance. *Journal of Experimental Botany* **45,** 179–186.

Zimmerman M.H. (1983) *Xylem Structure and the Ascent of Sap*. Springer-Verlag, Berlin, Germany.

Received 7 September 2010; received in revised form 26 October 2010; accepted for publication 28 October 2010